Acta Mechanica Sinica
DOI 10.1007/s10409-014-0062-5

RESEARCH PAPER

Folding of multi-layer graphene sheets Induced by van der Waals interaction

Xian-Hong Meng · Ming Li · Zhan Kang · Jian-Liang Xiao

Received: 18 September 2013 / Revised: 17 February 2014 / Accepted: 24 February 2014

Abstract Graphene sheets are extremely flexible, and thus small forces, such as van der Waals interaction, can induce significant out-of-plane deformation, such as folding. Folded graphene sheets show racket shaped edges, which can significantly affect the electrical properties of graphene. In this letter, we present combined theoretical and computational studies to reveal the folding behavior of multi-layer graphene sheets. A nonlinear theoretical model is established to determine the critical length of multilayer graphene sheets for metastable and stable folding, and to accurately predict the shapes of folded edges. These results all show good agreement with those obtained by molecular dynamics simulations.

Keywords Graphene · Folding · Stability · Theoretical model · Molecular dynamics simulation

1 Introduction

Graphene sheets show exceptional electronic and mechanical properties [1–7], and thus have many potential applications, such as nano-transistors, transparent electrodes, nano-electromechanical systems (NEMS), gas separation, desalination, nanocomposites and protection coatings [8–13]. Owing to their extreme flexibility, graphene sheets are susceptible to out-of-plane deformation. Recent studies show that suspended graphene sheets can fold and form folded edges due to van der Waals (vdW) interaction [14–16]. Similar folding and collapse behavior have also been observed in carbon nanotubes [17–20]. The folded edges of graphene sheets show racket shapes with structures similar to carbon nanotube walls, which can have strong influence on the electronic and magnetic properties of graphene [21–24]. Therefore, accurately predicting the critical length of graphene folding and the shapes of folded edges can be important for the application of graphene in nanoscale devices and systems.

A recent study by Cranford et al. [15] established a small deformation mechanics model to reveal the critical folding length of multi-layer graphene sheets. However, predicted shapes of the folded graphene edges was not given, partly because small deformation models cannot accurately predict the shapes of folded graphene edges. Meng et al. [16] developed a finite deformation theoretical model to study the folding of single-layer graphene, which can accurately predict not only the critical length of single-layer graphene folding but also the shape of the folded edge. However, the folding mechanics of multi-layer graphene sheets was not studied, and therefore it is not clear how the inter-layer interaction and the number of layers will affect the folding mechanics of graphene sheets.

In this work, we present combined theoretical analysis and molecular dynamics (MD) simulations to study the folding mechanics of multilayer graphene sheets. A theoretical model based on the finite deformation beam theory is developed, which can accurately predict the dependence of critical folding length on number of graphene layers. The shapes of folded edges of multi-layer graphene sheets are also given in analytical form. We have also conducted MD simulations to study the folding of multi-layer graphene sheets induced by vdW interactions. The results show good agreement with the theoretical model.

The project was supported by the National Natural Science Foundation of China (11172022 and 11302039) and the Major Project of Chinese National Programs for Fundamental Research and Development 2010CB832703.

X.-H. Meng
School of Aeronautic Science and Engineering,
Beihang University, 100191 Beijing, China

M. Li · Z. Kang
State Key Laboratory of Structural Analysis for
Industrial Equipment, Dalian University of Technology,
116024 Dalian, China
e-mail: mingli@dlut.edu.cn

J.-L. Xiao
Department of Mechanical Engineering,
University of Colorado, Boulder, CO 80309-0427, USA

2 Theoretical model

The schematic diagram of a folded double-layer graphene sheet is shown in Fig. 1a. The folded double-layer graphene consists of a curved region of length $2L$ and a flat region of length L_0. The total length of the folded double-layer graphene is $L_{\text{tot}} = 2(L + L_0)$. The equilibrium interlayer distance between any two closest graphene layers is d. The configuration of the folded graphene sheet results from the competition between adhesion energy U_{adhesion} in the flat region and bending energy U_{bending} in the curved region. If the flat graphene (as shown in Fig. 1b) is considered as the ground state, the energy of the folded graphene sheet (as shown in Fig. 1c) is $U_{\text{tot}} = U_{\text{bending}} + U_{\text{adhesion}}$. The adhesion energy $U_{\text{adhesion}} = -\gamma L_0$ with γ denoting the binding energy per unit area of graphene, and U_{bending} is to be determined later. If the graphene is too short, the total energy $U_{\text{tot}} > 0$, the resistance from the curved region can overcome the adhesion from the flat region, and therefore the folded graphene is unstable and can unfold. If the graphene is long enough, the total energy $U_{\text{tot}} > 0$, the adhesion energy over the flat region exceeds the resistance from the curved region, and therefore the folded graphene is energetically preferred and stable. Obviously, there exists a critical length $L_{\text{tot}}^{\text{critical}}$, which separates the stable and the unstable folded configurations of graphene.

For a multi-layer graphene sheet, each layer of the graphene can be modeled as a beam with a bending stiffness EI. Owing to symmetry, only the top half of the folded graphene will be analyzed. The interlayer distance is assumed to keep constant d, and the sliding between layers is free. The analytical model to be presented is based on the middle plane of the multilayer graphene sheet. This middle plane is a real graphene layer for a graphene sheet with odd number of layers, and is an imaginary plane for a graphene sheet with even number of layers (dash lines in Fig. 1a). The free-body diagram of a folded graphene is schematically illustrated in Fig. 2a. The normal force, shear force and bend-

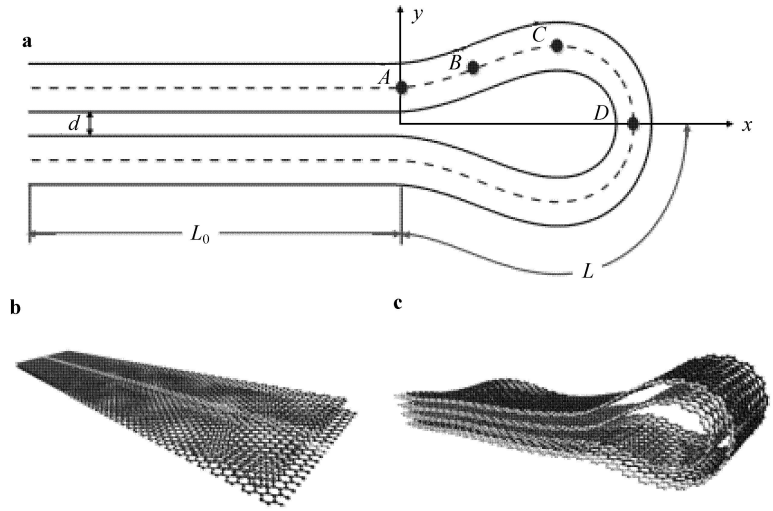

Fig. 1 **a** Schematic illustration of a folded double-layer graphene. The lengths of the flat and the curved regions are L_0 and L, respectively. The curved region is divided into three sections by four points, A, B, C, and D. The flat **b** and the folded **c** states of a double-layer graphene obtained from MD simulations

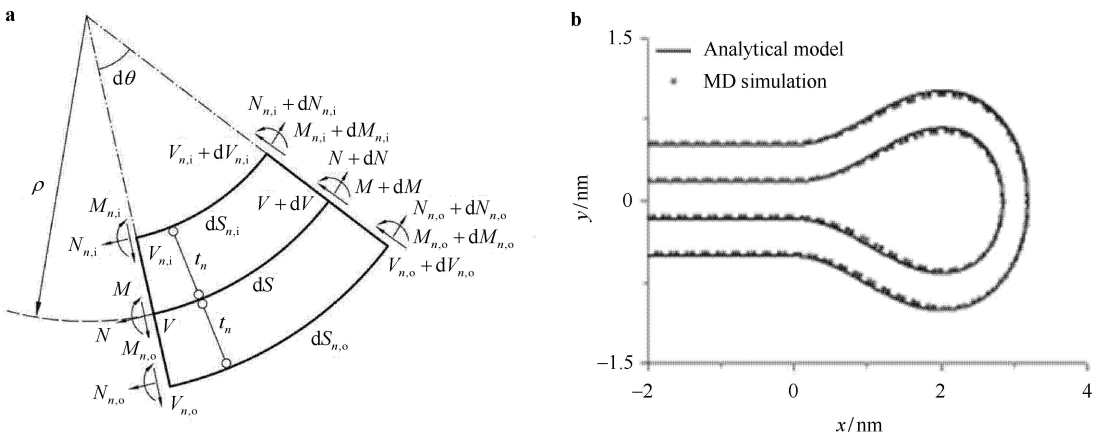

Fig. 2 Schematic illustration of the free-body diagram of a folded multi-layer graphene; **b** The comparison of profiles of a folded double-layer graphene given by the theoretical model and MD simulation

ing moment on the middle layer are denoted as N, V, and M, respectively. For the n-th inner layer, these internal forces are denoted as $N_{n,\mathrm{i}}$, $V_{n,\mathrm{i}}$, and $M_{n,\mathrm{i}}$. For the n-th outer layer, these internal forces are denoted as $N_{n,\mathrm{o}}$, $V_{n,o}$, and $M_{n,\mathrm{o}}$. The total number of layers of the graphene sheet is $J = 2j$ (for even number of layers) or $J = 2j+1$ (for odd number of layers). The distance between each layer (either inner or outer) and the middle plane is $t_n = (n - 0.5) \times d$ (for even number of layers) or $n \times d$ (for odd number of layers).

For the curved region, the curvature of the middle plane is $\kappa = 1/\rho = \mathrm{d}\theta/\mathrm{d}S$, where θ is the rotation angle and S is the arc length measured from point A, as shown in Fig. 1a. The curvatures for an inner and outer layer are $\kappa_{n,\mathrm{i}}$ and $\kappa_{n,\mathrm{o}}$, respectively. Four points, A, B, C, and D, divide the top half curved region into three sections, with A and D being the left most and right most points in the curved region of the graphene (with curvature κ_0 and rotation angle $\theta = 0$ at A, and curvature $-\kappa_1$ and rotation angle $\theta = -\pi/r\mathrm{d}2$ at D), C being the top most point of the curved region (with curvature $-\kappa_0$ and rotation angle $\theta = 0$), and B being a point between A and C, with curvature of 0 [16]. We first analyze a graphene sheet with odd number of layers, and then the results can be easily extended to a graphene sheet with even number of layers by taking the bending stiffness of the middle plane to be zero. Assuming that the total thickness of the multilayer graphene sheet $t = J \times d$ is much smaller than the radius of curvature of the curved region, since the interlayer distance is assumed to be constant, the curvatures for an inner layer and an outer layer can be obtained to the first-order approximation as

$$\kappa_{n,\mathrm{i}} = \frac{\mathrm{d}\theta}{\mathrm{d}S_{n,\mathrm{i}}} = \kappa(1 + t_n\kappa), \quad n = 1, 2, \cdots, j, \tag{1}$$

$$\kappa_{n,\mathrm{o}} = \frac{\mathrm{d}\theta}{\mathrm{d}S_{n,\mathrm{o}}} = \kappa(1 - t_n\kappa), \quad n = 1, 2, \cdots, j. \tag{2}$$

The bending moments of the middle, inner and outer layers are

$$M = EI\kappa, \tag{3}$$

$$M_{n,\mathrm{i}} = EI\kappa(1 + t_n\kappa), \tag{4}$$

$$M_{n,\mathrm{o}} = EI\kappa(1 - t_n\kappa). \tag{5}$$

With the help of Eqs. (1) and (2), the bending moment equilibrium equations for the middle, inner, and outer layers are obtained as

$$\frac{\mathrm{d}M}{\mathrm{d}S} = -V, \tag{6}$$

$$\frac{\mathrm{d}M_{n,\mathrm{i}}}{\mathrm{d}S_{n,\mathrm{i}}} = (1 + t_n\kappa)\frac{\mathrm{d}M_{n,\mathrm{i}}}{\mathrm{d}S} = -V_{n,\mathrm{i}}, \tag{7}$$

$$\frac{\mathrm{d}M_{n,\mathrm{o}}}{\mathrm{d}S_{n,\mathrm{o}}} = (1 - t_n\kappa)\frac{\mathrm{d}M_{n,\mathrm{o}}}{\mathrm{d}S} = -V_{n,\mathrm{o}}. \tag{8}$$

Summing up Eqs. (6)–(8) over all graphene layers yields an equilibrium equation for the multi-layer graphene as

$$\frac{\mathrm{d}\left[M + \sum_{n=1}^{j}(M_{n,\mathrm{i}} + M_{n,\mathrm{o}})\right]}{\mathrm{d}S} + \sum_{n=1}^{j} t_n\kappa\frac{\mathrm{d}}{\mathrm{d}S}(M_{n,\mathrm{i}} - M_{n,\mathrm{o}}) = -V - \sum_{n=1}^{j}(V_{n,\mathrm{i}} + V_{n,\mathrm{o}}). \tag{9}$$

Since the graphene sheet thickness is much smaller than the radius of curvature, $t_n\kappa < 1$, insering Eqs. (4) and (5) into Eq. (9) shows that the second term on the left-hand side of Eq. (9) is much smaller (to the order of $(t_n\kappa)^2$) than the first term, and therefore can be neglected. Then the bending moment equilibrium equation (9) changes to

$$\frac{\mathrm{d}M_t}{\mathrm{d}S} = -V_t, \tag{10}$$

where $M_t = M + \sum_{n=1}^{j}(M_{n,\mathrm{i}} + M_{n,\mathrm{o}}) = (2j+1)EI\kappa$ and $V_t = V + \sum_{n=1}^{j}(V_{n,\mathrm{i}} + V_{n,\mathrm{o}})$ are the total bending moment and total shear force, respectively. Please note that Eq. (10) also holds for a graphene sheet with even number of layers, therefore we have generally $M_t = JEI\kappa$.

The tangent direction force equilibrium equations of the middle plane, the n-th inner layer and outer layer are given as

$$\frac{\mathrm{d}N}{\mathrm{d}S} - V\frac{\mathrm{d}\theta}{\mathrm{d}S} = 0, \tag{11}$$

$$\frac{\mathrm{d}N_{n,\mathrm{i}}}{\mathrm{d}S_{n,\mathrm{i}}} - V_{n,\mathrm{i}}\frac{\mathrm{d}\theta}{\mathrm{d}S_{n,\mathrm{i}}} = 0, \tag{12}$$

$$\frac{\mathrm{d}N_{n,\mathrm{o}}}{\mathrm{d}S_{n,\mathrm{o}}} - V_{n,\mathrm{o}}\frac{\mathrm{d}\theta}{\mathrm{d}S_{n,\mathrm{o}}} = 0. \tag{13}$$

Multiplying both sides of Eq. (12) by $\mathrm{d}S_{n,\mathrm{i}}/\mathrm{d}S$ gives

$$\frac{\mathrm{d}N_{n,\mathrm{i}}}{\mathrm{d}S} - V_{n,\mathrm{i}}\frac{\mathrm{d}\theta}{\mathrm{d}S} = 0. \tag{14}$$

Similarly, multiplying both sides of Eq. (13) by $\mathrm{d}S_{n,\mathrm{o}}/\mathrm{d}S$ gives

$$\frac{\mathrm{d}N_{n,\mathrm{o}}}{\mathrm{d}S} - V_{n,\mathrm{o}}\frac{\mathrm{d}\theta}{\mathrm{d}S} = 0. \tag{15}$$

Summing up Eqs. (11), (14) and (15) for all layers gives

$$\frac{\mathrm{d}N_t}{\mathrm{d}S} - V_t\frac{\mathrm{d}\theta}{\mathrm{d}S} = 0, \tag{16}$$

where $N_t = N + \sum_{n=1}^{j}(N_{n,\mathrm{i}} + N_{n,\mathrm{o}})$ is the total normal force for the whole graphene sheet.

The radial direction equilibrium equation for the whole graphene sheet can also be obtained by summing up the equations on individual layers and is given as

$$\frac{\mathrm{d}V_t}{\mathrm{d}S} + N_t\frac{\mathrm{d}\theta}{\mathrm{d}S} = 0. \tag{17}$$

Equations (10), (16) and (17) consist of the equilibrium equations for multilayer graphene sheet folding, which are identical to those for single-layer graphene sheet folding, except that the bending stiffness EI of single-layer graphene is replaced by the bending stiffness of JEI of multi-layer graphene [16]. Therefore, the results for single-layer graphene folding from our previous study generally holds for multi-layer graphenes.

The deformed geometry of the graphene sheet can be completely described by two quantities, κ_0 and κ_1, with the Cartesian coordinates of any point in the curved region of the middle plane expressed as [16]

$$x = \begin{cases} \displaystyle\int_0^{\theta} \frac{\cos\theta}{\sqrt{\kappa_0^2 - (\kappa_1^2 - \kappa_0^2)\sin\theta}}\mathrm{d}\theta, & \text{in } AB, \\ \displaystyle\int_0^{\sin^{-1}\frac{\kappa_0^2}{\kappa_1^2-\kappa_0^2}} \frac{\cos\theta}{\sqrt{\kappa_0^2 - (\kappa_1^2 - \kappa_0^2)\sin\theta}}\mathrm{d}\theta + \int_{\theta}^{\sin^{-1}\frac{\kappa_0^2}{\kappa_1^2-\kappa_0^2}} \frac{\cos\theta}{\sqrt{\kappa_0^2 - (\kappa_1^2 - \kappa_0^2)\sin\theta}}\mathrm{d}\theta, & \text{in } BC, \\ \displaystyle 2\int_0^{\sin^{-1}\frac{\kappa_0^2}{\kappa_1^2-\kappa_0^2}} \frac{\cos\theta}{\sqrt{\kappa_0^2 - (\kappa_1^2 - \kappa_0^2)\sin\theta}}\mathrm{d}\theta - \int_0^{\theta} \frac{\cos\theta}{\sqrt{\kappa_0^2 - (\kappa_1^2 - \kappa_0^2)\sin\theta}}\mathrm{d}\theta, & \text{in } CD, \end{cases}$$

$$y = \begin{cases} \displaystyle\frac{Jd}{2} + \int_0^{\theta} \frac{\sin\theta}{\sqrt{\kappa_0^2 - (\kappa_1^2 - \kappa_0^2)\sin\theta}}\mathrm{d}\theta, & \text{in } AB, \\ \displaystyle\frac{Jd}{2} + \int_0^{\sin^{-1}\frac{\kappa_0^2}{\kappa_1^2-\kappa_0^2}} \frac{\sin\theta}{\sqrt{\kappa_0^2 - (\kappa_1^2 - \kappa_0^2)\sin\theta}}\mathrm{d}\theta + \int_{\theta}^{\sin^{-1}\frac{\kappa_0^2}{\kappa_1^2-\kappa_0^2}} \frac{\sin\theta}{\sqrt{\kappa_0^2 - (\kappa_1^2 - \kappa_0^2)\sin\theta}}\mathrm{d}\theta, & \text{in } BC, \\ \displaystyle\frac{Jd}{2} + 2\int_0^{\sin^{-1}\frac{\kappa_0^2}{\kappa_1^2-\kappa_0^2}} \frac{\sin\theta}{\sqrt{\kappa_0^2 - (\kappa_1^2 - \kappa_0^2)\sin\theta}}\mathrm{d}\theta - \int_0^{\theta} \frac{\sin\theta}{\sqrt{\kappa_0^2 - (\kappa_1^2 - \kappa_0^2)\sin\theta}}\mathrm{d}\theta, & \text{in } CD, \end{cases} \tag{18}$$

where $\theta = -\sin^{-1}\dfrac{\kappa^2 - \kappa_0^2}{\kappa_1^2 - \kappa_0^2}$. The governing equations for determining κ_0 and κ_1 are [16]

$$L = \int_0^{\frac{\pi}{2}} \frac{1}{\sqrt{\kappa_0^2 + \sin\theta(\kappa_1^2 - \kappa_0^2)}}\mathrm{d}\theta + 2\int_0^{\sin^{-1}\frac{\kappa_0^2}{\kappa_1^2-\kappa_0^2}} \frac{1}{\sqrt{\kappa_0^2 - \sin\theta(\kappa_1^2 - \kappa_0^2)}}\mathrm{d}\theta, \tag{19}$$

$$\frac{t}{2} = -2\int_0^{\sin^{-1}\frac{\kappa_0^2}{\kappa_1^2-\kappa_0^2}} \frac{\sin\theta}{\sqrt{\kappa_0^2 - (\kappa_1^2 - \kappa_0^2)\cos\theta}}\mathrm{d}\theta + \int_0^{\frac{\pi}{2}} \frac{\sin\theta}{\sqrt{\kappa_0^2 + (\kappa_1^2 - \kappa_0^2)\cos\theta}}\mathrm{d}\theta, \tag{20}$$

which can be solved numerically.

The bending energy in the curved region U_{bending} is obtained to its first order approximation as

$$U_{\text{bending}} = 2JEI\int_0^{\sin^{-1}\frac{\kappa_0^2}{\kappa_1^2-\kappa_0^2}} \sqrt{\kappa_0^2 - (\kappa_1^2 - \kappa_0^2)\sin\theta}\mathrm{d}\theta + JEI\int_0^{\frac{\pi}{2}} \sqrt{\kappa_0^2 + (\kappa_1^2 - \kappa_0^2)\sin\theta}\mathrm{d}\theta. \tag{21}$$

The total energy of the folded graphene sheet is given as

$$U_{\text{tot}} = U_{\text{bending}} - \frac{\gamma}{2}(L_{\text{tot}} - 2L), \tag{22}$$

which is a function of the curved region length L only. Minimization of Eq. (22) gives solution to the folding of multi-layer graphene sheet, which can be solved by numerical methods.

3 Molecular dynamics simulation

Molecular dynamics (MD) simulations have been performed to study the folding of multi-layer graphene sheets, and to verify the theoretical model. Large-scale molecular simulation package LAMMPS [25] was used to conduct the simulations, and visualization program VMD [26] was used to analyze the results. The adaptive intermolecular reactive empirical bond order (AIREBO) potential [27] was adopted to model the C—C atomic interactions, with the short-range C—C bonding characterized by the reactive empirical bond order (REBO) term [28] and the long-range van der Waals interaction characterized by Lennard–Jones (LJ) term. The parameters for LJ interaction were set to be $\varepsilon = 2.4$ meV, $\sigma = 0.34$ nm [16, 20] and the cut-off distance = 1.05 nm.

In the MD simulations, a rectangular double-layer graphene sheet of length of 20 nm and width of 5 nm, as

shown in Fig. 1b, was firstly adopted to study the folding of double-layer graphene. To make the left end of folded graphene aligned, the top layer graphene was cut to be shorter than the bottom layer by around 0.6 nm. To avoid thermal oscillation, a constant temperature of 0 K was adopted during the simulations. To create folded graphene sheets, the two ends of the flat graphene shown in Fig. 1b were brought together by external loads, and then the graphene was fully relaxed after the external loads were removed. A folded double-layer graphene is shown in Fig. 1c. The folded graphene clearly shows a racket shape. To find the critical length of stable folding, different lengths were used in MD simulations. For the folding of other multi-layer graphene sheets, similar protocols were used to create the folding and to relax the system.

4 Results and discussion

In the analytical model, the bending stiffness of each graphene layer and interlayer spacing are $EI = 1.4\,\mathrm{eV}$ and $d = 0.34\,\mathrm{nm}$, respectively, and the adhesion energy per unit area between two closest graphene layers is $\gamma_0 = 1.45\,\mathrm{eV/nm^2}$ [29–33]. However, for multilayer graphene folding, the second closest graphene layer also contributes to the adhesion energy. Since the adhesion energy is related to interlayer distance to the order of −4 [34], the adhesion energy for multilayer graphene folding is obtained as $\gamma = (9/8)\gamma_0 = 1.63\,\mathrm{eV/nm^2}$. The profiles of a folded double-layer grpahene obtained from the theoretical model and MD simulation are depicted in Fig. 2b, which show good agreement.

The total energies of folded double-layer graphene sheets versus the half length of curved region L are shown in Fig. 3a for different total graphene lengths. The dots mean that the curved region half length L reaches $L_{\mathrm{tot}}/2$. Figure 3a shows that the curved region reaches optimal state when $L = 4\,\mathrm{nm}$, which is larger than 2.5 nm, the value for the optimal state of single-layer graphene folding. For graphene sheets longer than 8 nm, there exists a minimal energy point on the curve, which corresponds to the optimal folded state. When the graphene sheet is not long enough, this minimal energy $U_{\mathrm{tot}} > 0$, which means that the folded configuration is metastable and can unfold to flat configuration when the system is subject to perturbation. As the total length of the graphene L_{tot} increases, the total system energy U_{tot} decreases. When the length of the graphene sheet exceeds a critical value $L^{\mathrm{c}}_{\mathrm{tot}} = 15.46\,\mathrm{nm}$, the minimal energy $U_{\mathrm{tot}} < 0$, which means that the folded graphene is more stable than the flat configuration. The dependence of the critical folding length $L^{\mathrm{c}}_{\mathrm{tot}}$ on the graphene layer number is also studied and shown in Fig. 3b. The critical folding length increases with the number of layers. This is because the bending stiffness and bending energy of the multi-layer graphene increase with increasing number of layers. To compensate for the increased bending energy of the curved region, longer flat region is required to provide enough adhesion energy to resist the unfolding.

MD simulations have also been conducted to study the stability of double-layer graphene folding. Double-layer graphene sheets with different lengths are folded and then fully relaxed. The energy differences between the folded and the flat configurations for each length are plotted versus the length in Fig. 4a, which is named as a stability map for double-layer graphene folding. The stability map suggests two critical lengths which divide the double-layer graphene folding into three regimes: (1) For $L_{\mathrm{tot}} < 9\,\mathrm{nm}$, only flat configuration is stable, the folded graphene unfolds autonomously after relaxation; (2) For $9\,\mathrm{nm} < L_{\mathrm{tot}} < 13\,\mathrm{nm}$, the folded graphene is metastable, enough perturbation can unfold the folded graphene sheet; (3) For $L_{\mathrm{tot}} > 13\,\mathrm{nm}$, the folded configuration is more stable than the flat graphene, with enough perturbation, the flat graphene would fold by itself. Figure 4b shows configurations of double-layer graphene sheets for each of the three regimes, i.e., flat stable, folded metastable and folded stable.

In addition to double-layer graphene, the folded configurations for other multi-layer graphene sheets are also obtained. Figure 5 shows the folded profiles for 3-, 4-, 6-, and 8-layer graphene sheets. The solid lines are obtained by theoretical model, and the dashed lines are from MD simulations. The profiles predicted by the theoretical model show excellent agreement with those from MD simulations for all graphene sheets.

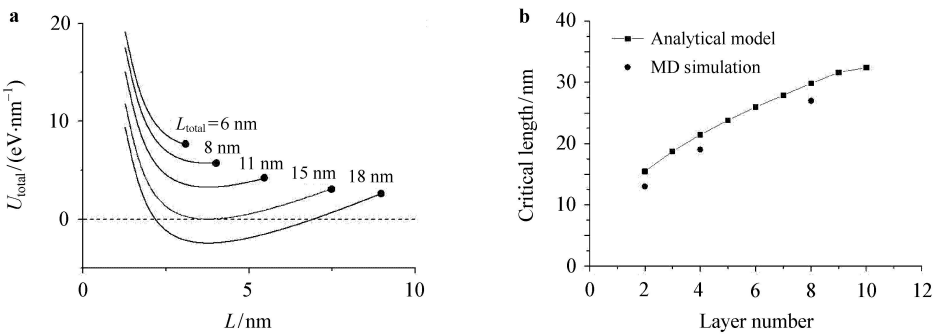

Fig. 3 **a** The total energies of folded double-layer graphene sheets versus the half length of curved region L, for different total graphene lengths. The dots mean that the curved region half length L reaches $L_{\mathrm{tot}}/2$; **b** The critical folding length of multi-layer graphene sheet versus the number of graphene layers

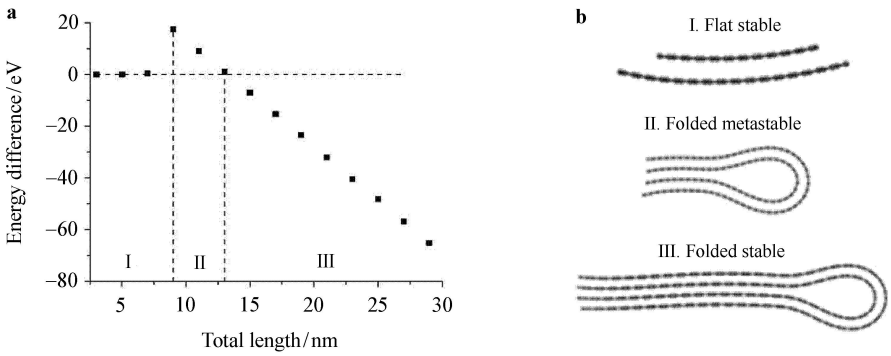

Fig. 4 **a** Stability map for double-layer graphene folding, which suggests two critical lengths to divide the double-layer graphene folding into three regimes, i.e., unfold stable, folded metastable and folded stable; **b** Configurations of double-layer graphene sheets for each of the three regimes

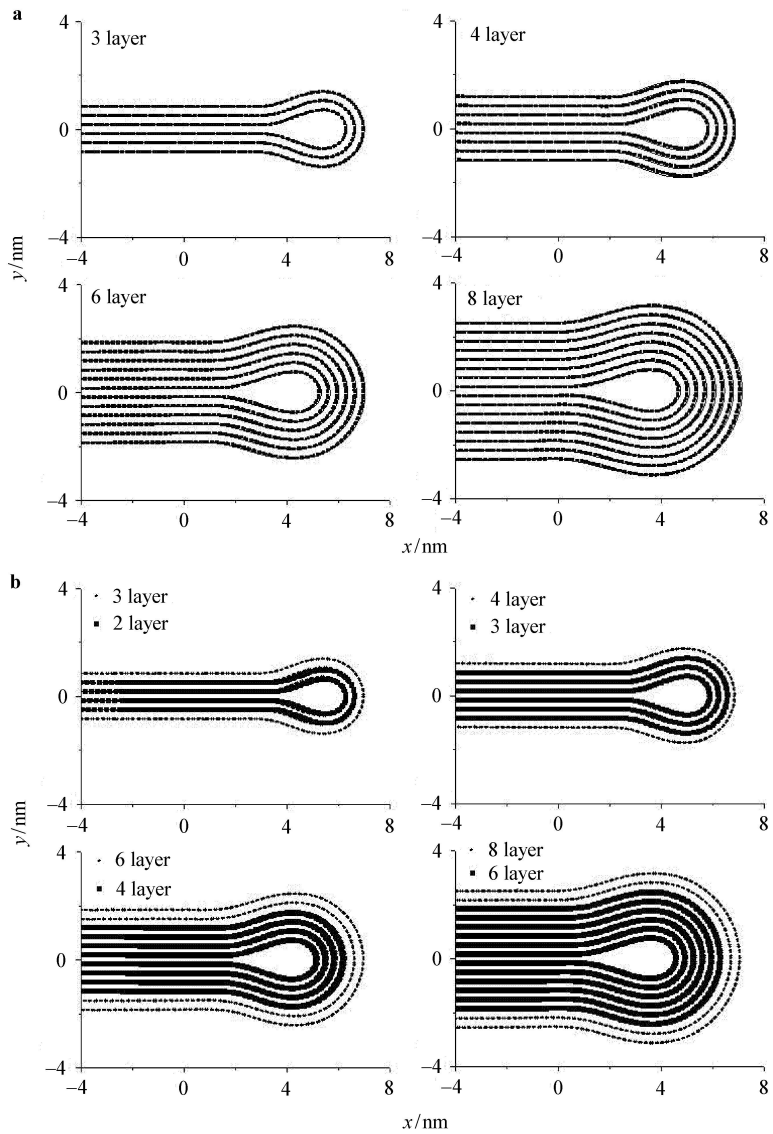

Fig. 5 **a** Profiles of folded multi-layer graphene sheets with 3, 4, 6, and 8 graphene layers. The solid lines are from theoretical model, and the dashed lines are from MD simulations; **b** Profile comparison between different number of layers

It should be pointed out that the bending rigidity is supposed to be linear and the interlayer frictional shear is neglected in this paper. However, previous studies showed that the bending rigidity of few-layer graphene can be affected by interlayer shear and its value is not necessarily linear for thicker graphene samples [35–38]. The above simplified model would not be effective for thicker graphene samples. However, from the results, the supposition is valid when there are only a few layers. But with the increase of the number of layers, the difference between analytical method and the MD method is getting greater which can be seen from the comparative result of 8 layers.

In our analytical model, the assumption $t_n\kappa < 1$ is used and a much smaller $(t_n\kappa)^2$ is neglected. Actually in some parts of curved region the assumption may not hold, but the final result is got from the minimization of the total energy. When the assumption $t_n\kappa < 1$ holds within a large part of the curved region, the energy difference caused by the small part where the assumption does not hold would be very small compared to the total energy, and then the error of the final result would be tiny. With the increase of the number of layers, the assumption would not hold in a large part of the curved region and then the model would be ineffective. It is the same for the supposition of the linear bending rigidity. To summarize, the analytical model is effective when there are a few layers of graphene, but invalid when there are many layers, and then a new theoretical model should be set up to analyze.

5 Conclusions

A finite deformation theoretical model is developed to study the folding of multi-layer graphene sheets. The critical length for stable folding and the folded profile can be accurately predicted, which show good agreement with MD simulation results. The agreement also validates the assumption that the interlayer friction between graphene layers can be neglected for this kind of deformation. The results can find applications in the design and fabrication of grpahene-based nanoscale devices and systems.

Acknowledgements J. Xiao also acknowledges the startup support from the College of Engineering and Applied Science of University of Colorado Boulder.

References

1 Bunch, J.S., van der Zande, A.M., Verbridge, S.S., et al.: Electromechanical resonators from graphene sheets. Science **315**, 490–493 (2007)
2 Meyer, J.C., Geim, A.K., Katsnelson, M.I., et al.: The structure of suspended graphene sheets. Nature **446**, 60–63 (2007)
3 Neto, A.H.C., Guinea, F., Peres, N.M.R., et al.: The electronic properties of graphene. Reviews of Modern Physics **81**, 109 (2009)
4 Lee, C., Wei, X., Kysar, J.W., et al.: Measurement of the elastic properties and intrinsic strength of monolayer graphene. Science **321**, 385–388 (2008)
5 Geim, A.K., Novoselov, K.S.: The rise of graphene. Nature materials **6**, 183–91 (2007)
6 Zhu, Y., Murali, S., Cai, W., et al.: Graphene and graphene oxide: synthesis, properties, and applications. Advanced Materials **22**, 3906–3924 (2010)
7 Li, X., Cai, W., An, J., et al.: Large-area synthesis of high-quality and uniform graphene films on copper foils. Science **324**, 1312–1314 (2009)
8 Zhu, Y., Murali, S., Stoller, M.D., et al.: Carbon-based supercapacitors produced by activation of graphene. Science **332**, 1537–1541 (2011)
9 Bunch, J.S., Verbridge, S.S., Alden, J. S., et al.: Impermeable atomic membranes from graphene sheets. Nano Letters **8**, 2458–2462 (2008)
10 Koenig, S.P., Boddeti, N.G., Dunn, M.L., et al.: Ultrastrong adhesion of graphene membranes. Nature Nanotechnology **6**, 543–546 (2011)
11 Koenig, S.P., Wang, L., Pellegrino, J., et al.: Selective molecular sieving through porous graphene. Nature Nanotechnology **7**, 728–732 (2012)
12 Weiss, N.O., Zhou, H., Liao, L., et al.: Graphene: An emerging electronic material. Advanced Materials **24**, 5782–5825 (2012)
13 Novoselov, K.S., Fal, V.I., Colombo, L., et al.: A roadmap for graphene. Nature **490**, 192–200 (2012)
14 Zhang, J., Xiao, J., Meng, X., et al.: Free folding of suspended graphene sheets by random mechanical stimulation. Physical Review Letters **104**, 166805 (2010)
15 Cranford, S., Sen, D., Buehler, M.J. Meso-origami: Folding multilayer graphene sheets. Applied Physics Letters **95**, 123121 (2009)
16 Meng, X., Li, M., Kang, Z., et al.: Mechanics of self-folding of single-layer graphene. Journal of Physics D: Applied Physics **46**, 055308 (2013)
17 Zhou, W., Huang, Y., Liu, B., et al.: Self-folding of single- and multiwall carbon nanotubes. Applied Physics Letters **90**, 073107 (2007)
18 Buehler, M.J., Kong, Y., Huang, Y., et al.: Self-folding and unfolding of carbon nanotubes. Journal of Engineering Materials and Technology **128**, 3–10 (2006)
19 Xiao, J., Liu, B., Huang, Y., et al.: Stability and chirality effect on twist formation of collapsed double wall carbon nanotubes. Transactions of Nonferrous Metals Society of China **16**, s776–s779 (2006)
20 Xiao, J., Liu, B., Huang Y, et al.: Collapse and stability of single-and multi-wall carbon nanotubes. Nanotechnology **18**, 395703 (2007)
21 Son, Y.W., Cohen, M.L., Louie, S. G.: Energy gaps in graphene nanoribbons. Physical Review Letters **97**, 216803 (2006)
22 Nakada, K., Fujita, M., Dresselhaus, G., et al.: Edge state in graphene ribbons: Nanometer size effect and edge shape dependence. Physical Review B **54**, 17954 (1996)
23 Enoki, T., Kobayashi, Y., Fukui, K.I.: Electronic structures of graphene edges and nanographene. International Reviews in Physical Chemistry **26**, 609–645(2007)
24 Ritter, K.A., Lyding, J.W.: The influence of edge structure on the electronic properties of graphene quantum dots and nanoribbons. Nature Materials **8**, 235–242 (2009)
25 Plimpton, S.: Fast parallel algorithms for short-range molecular dynamics. Journal of Computational Physics **117**, 1–19 (1995)

26 Humphrey, W., Dalke, A., Schulten, K.: VMD: Visual molecular dynamics. Journal of Molecular Graphics **14**, 33–38 (1996)
27 Stuart, S.J, Tutein, A.B, Harrison, J.A.: A reactive potential for hydrocarbons with intermolecular interactions. The Journal of Chemical Physics **112**, 6472–6486 (2000)
28 Brenner, D.W, Shenderova, O.A, Harrison, J.A, et al.: A second-generation reactive empirical bond order (REBO) potential energy expression for hydrocarbons. Journal of Physics: Condensed Matter **14**, 783 (2002)
29 Huang, Y., Wu, J., Hwang, K.C.: Thickness of graphene and single-wall carbon nanotubes. Physical Review B **74**, 245413 (2006)
30 Liu, B., Yu, M.F, Huang, Y.: Role of lattice registry in the full collapse and twist formation of carbon nanotubes. Physical Review B **70**, 161402 (2004)
31 Girifalco, L.A, Hodak, M., Lee, R.S.: Carbon nanotubes, buckyballs, ropes, and a universal graphitic potential. Physical Review B **62**, 13104 (2000)
32 Zhang, D.B, Akatyeva, E., Dumitrică T.: Bending ultrathin graphene at the margins of continuum mechanics. Physical Review Letters **106**, 255503 (2011)
33 Kudin, K.N., Scuseria, G.E., Yakobson, B.I.: C2F, BN, and C nanoshell elasticity from ab initio computations. Physical Review B **64**, 235406 (2001)
34 Sarabadani, J., Naji, A., Asgari, R., et al.: Many-body effects in the van der Waals–Casimir interaction between graphene layers. Physical Review B **84**, 155407 (2011)
35 Poot, M., van der Zant, H.S.J.: Nanomechanical properties of few-layer graphene membranes. Applied Physics Letters **92**, 063111 (2008)
36 Liu, Y., Xu, Z., Zheng, Q.: The interlayer shear effect on graphene multilayer resonators. Journal of the Mechanics and Physics of Solids **59**, 1613–1622 (2011)
37 Zakharchenko, K.V., Los, J.H., Katsnelson, M.I., et al.: Atomistic simulations of structural and thermodynamic properties of bilayer graphene. Physical Review B **81**, 235439 (2010)
38 Kang, J.W, Lee, S.: Molecular dynamics study on the bending rigidity of graphene nanoribbons. Computational Materials Science **74**, 107–113 (2013)